Reprinted from SPIE Vol. 828—Digital Image Recovery and Synthesis

Invited Paper

Speckle imaging techniques

J C. Dainty

Blackett Laboratory, Imperial College, London SW7 2BZ, UK

ABSTRACT

Several proposed techniques of focal plane imaging through turbulence are described and compared. The techniques are: shift-and-add, exponential filter, Knox-Thompson (cross-spectrum) and triple correlation. Particular attention is given to the performance of the methods at extremely low light levels of a few detected photons per frame.

INTRODUCTION

Speckle interferometry, as invented by Labeyrie[1], provides an estimate of the diffraction limited autocorrelation or energy spectrum of an object. In a linear, isoplanatic, incoherent imaging system, the image intensity $i(\underline{x})$ is related to the object intensity $o(\underline{x})$ by a convolution relationship,

$$i(\underline{x}) \quad = \quad o(\underline{x}) * p(\underline{x}) \ , \tag{1}$$

where * denotes convolution and $p(\underline{x})$ is the instantaneous point spread function of the optical system. When imaging through turbulence, $p(\underline{x})$ is a random speckle pattern whose statistics are similar to those of laser speckle patterns[2]. In Fourier space, Eq.(1) is

$$I(\underline{u}) \quad = \quad O(\underline{u}) \ . \ P(\underline{u}) \ , \tag{2}$$

where the upper-case functions denote the Fourier transforms of the lower-case ones; the quantity $P(u)$ is the instantaneous telescope-atmosphere transfer function.

In conventional long-exposure imaging, one forms the average,

$$\langle I(\underline{u}) \rangle \quad = \quad O(\underline{u}) \ . \langle P(\underline{u}) \rangle \tag{3}$$

and, as is well-known, the average telescope-atmosphere transfer function $\langle P(\underline{u}) \rangle$ drops off rapidly for angular spatial frequencies greater than r_o/λ, where r_o, the Fried parameter, is typically 10 cm at a good observing site.

In speckle interferometry, one forms an average of the energy spectrum,

$$\begin{aligned} \langle I^{(2)}(\underline{u}) \rangle \quad &= \quad \langle I(\underline{u}) \ I^*(\underline{u}) \rangle \\ &= \quad O^{(2)}(\underline{u}) \ . \langle P^{(2)}(\underline{u}) \rangle . \end{aligned} \tag{4}$$

In Eq.(4), the superscript $^{(2)}$ denotes that a second order correlation is being performed, which in image space could be written

$$\langle i^{(2)}(\underline{x}_1) \rangle \quad = \quad \langle \int_{-\infty}^{\infty} i(\underline{x}) \ i(\underline{x} + \underline{x}_1) \ d\underline{x} \rangle \ . \tag{5}$$

As originally shown by Korff [3], the speckle transfer function $\langle P^{(2)}(\underline{u}) \rangle$ contains a diffraction-limited component and thus allows the estimation of the energy spectrum of the object up to an angular spatial frequency of D/λ, where D is the telescope diameter.

As a result of Eq (4), speckle interferometry has three properties that have contributed significantly to its success in astronomy:

(i) it provides diffraction-limited information about the object structure ,
(ii) that information is perturbed by a <u>linear</u> transfer function, and
(iii) the image energy spectrum can be evaluated at very low light levels using

photon correlation techniques [4].

Regarding point (ii), it is not essential that the transfer process be linear, but it is usually desirable and in any case the imaging process must be well-understood and have an inverse solution so that object data can be found quantitatively.

Clearly, neither Eq.(4) or (5), provides an estimate of the object map $o(\underline{x})$ directly. Methods of trying to estimate $o(\underline{x})$ from its energy spectrum $O^{(2)}(\underline{u})$ are reviewed in these Proceedings by Fienup and elsewhere[5]. The problem is that of estimating the phase $\varphi(\underline{u})$ of $O(\underline{u})$, given the squared modulus $O^{(2)}(\underline{u}) = |O(\underline{u})|^2$. Although a considerable amount of effort has gone into solving this problem, no general solution exists. Furthermore, speckle patterns contain information that is additional to that given by the energy spectrum and this should be exploited when finding the object map.

In the following section we review briefly four proposed methods of speckle imaging, each of which processes the raw speckle data in a different way to Labeyrie's speckle interferometry. However, it is desirable that any proposed technique of speckle imaging retains the advantageous properties (i) - (iii) of the original speckle technique, as well as giving an estimate of the object map. Property (iii), the ability to work at very low light levels, is particularly important, since just about any method works when photon noise is neglected.

FOUR PROPOSED TECHNIQUES OF SPECKLE IMAGING

A. Shift-and-add

In this method, first proposed by Lynds et al[6] and considerably extended by Bates[7-9] and others[10], one averages centroided versions of selected bright speckles. At high light levels, the method would have linear transfer function if each "speckle" were a randomly translated, linearly degraded image of the original object. This is not the case, as shown by Hunt et al[11], and the shift-and-add method is not linear at high light levels. There is also the problem of identifying bright speckles in photon-limited data.

Recently, we have analysed shift-and-add imaging at very low light levels for the case of a randomly translating object[12] (whose imaging is linear at high light levels). The photon-limited case is also fundamentally non-linear. If $\langle Q_N(\underline{u}) \rangle$ denotes the Fourier spectrum of the average of all centroided frames that contain exactly N detected photons and $I(\underline{u})$ denotes the normalised Fourier spectrum of the high light level intensity of the original (unshifted) image, then

$$\langle Q_N(\underline{u}) \rangle = N \; I\left(\frac{N-1}{N} . \underline{u}\right) \left[I^* \left(\frac{\underline{u}}{N}\right)\right]^{N-1} \tag{6}$$

Thus, for example, for N = 2

$$\langle Q_2(\underline{u}) \rangle = 2 \; \left| \; I\left(\frac{\underline{u}}{2}\right) \right|^2 ; \tag{7}$$

that is, the spectrum of the shift-and-add image is proportional to the energy spectrum of the true image[12]. Equation (6) has interesting implications for phase retrieval[12].

B. Exponential filtering

For modulus-only reconstruction in one dimension, the solution is ambiguous because the complex zeros of the energy spectrum of the object include both the zeros of the original object and their inverses. The object can be reconstructed uniquely if its zeros can be identified correctly and Walker[13,14] showed that this can be done using an exponential filter in the image domain.

The average energy spectrum of the image, $\langle I^{(2)}(\underline{u}) \rangle = \langle |I(\underline{u})|^2 \rangle$, is found in the usual way. A second energy spectrum $\langle I'^{(2)}(\underline{u}) \rangle$, is found by multiplying each frame $i(\underline{x})$ by an exponential , $\exp(-2\pi ax)$, where 'a' is a constant. It can be shown that

$$\langle I'^{(2)}(\underline{u}) \rangle = O'^{(2)}(\underline{u}) . \langle P'^{(2)}(\underline{u}) \rangle , \tag{8}$$

so that from the original data we can extract the energy spectrum of the object and that of the exponentially filtered object. In principle, these together contain sufficient information to reconstruct the object intensity. In practice, one has to use a modified version of the Fienup algorithm[5] to recover the object map and no satisfactory modification exists.

C. Cross-spectrum method

This method was first proposed by Knox and Thompson[15] (KT). The KT correlation, $i^{(KT)}(\underline{x}_1,\Delta\underline{u})$, and its Fourier transform (with respect to $\underline{x}_1$), $I^{(KT)}(\underline{u}_1,\Delta\underline{u})$, are defined by

$$i^{(KT)}(\underline{x}_1,\Delta\underline{u}) = \int_{-\infty}^{\infty} i^*(\underline{x})\ i(\underline{x}+\underline{x}_1)\ \exp(2\pi i\Delta\underline{u}.\underline{x})\ d\underline{x} \tag{9}$$

and

$$I^{(KT)}(\underline{u}_1,\Delta\underline{u}) = I(\underline{u}_1)\ I^*(\underline{u}_1+\Delta\underline{u}), \tag{10}$$

where $\Delta\underline{u}$ is a fixed small vector.

When applying Eqs.(9) and (10) to speckle imaging, an average is taken over many speckle frames and it can be shown that[4]

$$\langle I^{(KT)}(\underline{u}_1,\Delta\underline{u})\rangle = O^{(KT)}(\underline{u}_1,\Delta\underline{u})\ .\ \langle P^{(KT)}(\underline{u}_1,\Delta\underline{u})\rangle, \tag{11}$$

where $$O^{(KT)}(\underline{u}_1,\Delta\underline{u}) = O(\underline{u}_1)\ O^*(\underline{u}_1+\Delta\underline{u}) \tag{12}$$

and $$\langle P^{(KT)}(\underline{u}_1,\Delta\underline{u})\rangle \approx \langle P^{(2)}(\underline{u}_1)\rangle\ .\ |\langle P(\tfrac{\Delta\underline{u}}{2})\rangle|^2, \tag{13}$$

where $\langle P\rangle$ is the seeing-limited transfer function. It follows from Eq (13) that $|\Delta\underline{u}|$ must be less than the seeing-limited angular frequency of r_o/λ for diffraction-limited information to be retained in Eq.(11). It also follows that the phase of the KT transfer function is zero and thus, taking the argument of Eq (11),

$$\varphi^{(KT)}(\underline{u}_1,\Delta\underline{u}) = \varphi_o(\underline{u}_1) - \varphi_o(\underline{u}_1+\Delta\underline{u}), \tag{14}$$

where $\varphi^{(KT)}$ is the phase of $I^{(KT)}$ and $\varphi_o(\underline{u})$ is the phase of $O(\underline{u})$.

Thus the KT technique gives phase difference information in the spectrum of the object and the phase has to be found by integration[16,17], avoiding phase dislocations.

D. Triple correlation

This method was first applied to speckle imaging by Weigelt[18-20] and is described in more detail elsewhere in these Proceedings and in reviews[4,5,21]. The triple (auto-) correlation and its Fourier transform, the bispectrum, are defined by

$$i^{(3)}(\underline{x}_1,\underline{x}_2) = \int_{-\infty}^{\infty} i^*(\underline{x})\ i(\underline{x}+\underline{x}_1)\ i(\underline{x}+\underline{x}_2)\ d\underline{x} \tag{15}$$

and

$$I^{(3)}(\underline{u}_1,\underline{u}_2) \;=\; I(\underline{u}_1)\, I^*(\underline{u}_1 + \underline{u}_2)\, I(\underline{u}_2) \; . \tag{16}$$

In speckle imaging, the average bispectrum of the image is related to that of the object through a bispectrum transfer function $\langle P^{(3)}(\underline{u}_1,\underline{u}_2) \rangle$,

$$\langle I^{(3)}(\underline{u}_1,\underline{u}_2) \rangle \;=\; O^{(3)}(\underline{u}_1,\underline{u}_2) \,.\, \langle P^{(3)}(\underline{u}_1,\underline{u}_2) \rangle \tag{17}$$

As with the KT technique, the bispectrum transfer function is non-zero in magnitude and has zero phase up to the diffraction limit of the telescope. Using this fact and taking the argument of Eq.(16), we find that

$$\varphi^{(3)}(\underline{u}_1,\underline{u}_2) \rangle \;=\; \varphi_o(\underline{u}_1) - \varphi_o(\underline{u}_1 + \underline{u}_2) + \varphi_o(\underline{u}_2) \; , \tag{18}$$

where $\varphi^{(3)}$ is the bispectrum phase. A recursive algorithm can be used to reconstruct the phase of the object transform, $\varphi_o(\underline{u})$, from the bispectrum phase.

COMPARISON OF CROSS-SPECTRUM AND BISPECTRUM

If Eq.(16) for the bispectrum of a single frame is written with $\underline{u}_2 = \Delta\underline{u}$, then, for a single 'plane' of the bispectrum,

$$\begin{aligned} I^{(3)}(\underline{u}_1,\Delta\underline{u}) &= I(\underline{u}_1)\, I^*(\underline{u}_1 + \Delta\underline{u})\, I(\Delta\underline{u}) \\ &= I^{(KT)}(\underline{u}_1,\Delta\underline{u})\, I(\Delta\underline{u}) \; , \end{aligned} \tag{19}$$

and thus this plane of the bispectrum equals the cross-spectrum multiplied by an image-dependent number $I(\Delta\underline{u})$ Taking the argument of Eq (19),

$$\varphi^{(3)}(\underline{u}_1,\Delta u) \;=\; \varphi^{(KT)}(\underline{u}_1,\Delta\underline{u}) + \varphi(\Delta\underline{u}) \tag{20}$$

The phase of the bispectrum is invariant to a translation of the image (this is clear from Eqs.(15) and (16)) whereas that of the cross-spectrum is not shift-invariant . When implementing the KT algorithm in practice, it is necessary to centroid each frame prior to processing and this is equivalent, in the noise sense, of calculating a single plane of the bispectrum.

Exact analytical expressions for the KT and bispectrum transfer functions are difficult to obtain and instead we have used Monte Carlo techniques to compare them. Figure 1 compares the two transfer functions for equivalent subplanes for realistic atmospheric parameters.

Signal-to-Noise Ratios

Both the cross-spectrum and triple correlation are complex quantities and thus both the signal-to-noise ratio of the modulus, SNR_m, and the phase error E_φ are of interest. The method of Goodman and Belsher[23] for finding SNR_m for the energy spectrum can be extended to the cross-spectrum and bispectrum for both SNR_m and E_φ[22]. Figure 2 shows SNR_m and E_φ in the frequency domain for an asteroid type of object and an imaging system with a unit transfer function (i e. no atmospheric turbulence), for a mean number N = 100 photons per frame for equivalent cross-spectrum (KT) and bispectrum sections. Note that the SNR_m is lower (and E_φ higher) for the bispectrum case, confirming the general result that errors are always higher on higher moments.

Note that, in practice,

$$E_\varphi \;\approx\; \frac{1}{\sqrt{2}\, SNR_m} \; , \tag{21}$$

as assumed by Nisenson and Papaliolios[24] in their analysis of the effect of photon noise on the KT algorithm.

In the presence of atmospheric turbulence, the expressions for the signal-to-noise ratio per frame in the cross-spectrum and bispectrum can become quite complicated[22]. At high light levels, then

$$\begin{aligned} &SNR^{(TC)} \sim 1 , && |\underline{u}_2| < r_o/\lambda \\ \text{and} \\ &SNR^{(KT)} \sim 1 . && |\Delta\underline{u}| < r_o/\lambda \end{aligned} \tag{22}$$

For $|\Delta\underline{u}| >> r_o/\lambda$, $SNR^{(KT)} \approx 0$, whereas for $|\underline{u}_2| >> r_o/\lambda$,

$$SNR^{(TC)} \approx \frac{2T^{(3)}(\underline{u}_1,\underline{u}_2)}{n_s\ T^{(2)}(\underline{u}_1)\ T^{(2)}(\underline{u}_1+\underline{u}_2)\ T^{(2)}(\underline{u}_2)} , \tag{23}$$

where $T^{(n)}$ is the normalised overlap area of n pupils.

At low light levels, in the important region $|\Delta\underline{u}|$ and $|\underline{u}_2| < r_o/\lambda$, both signal-to-noise ratios show a linear dependence on the average number of photons per speckle, just like the power spectrum case. For $|\Delta\underline{u}|$ and $|\underline{u}_2| >> r_o/\lambda$, the cross-spectrum has a signal-to-noise of essentially zero, whereas the bispectrum maintains a small value which is strongly dependent on the average number of speckles per frame.

ACKNOWLEDGEMENTS

I am grateful to G R Ayers, L C de Freitas and M J Northcott for their contributions to this and related work, which is supported by Grant GR/D 92332 from the UK Science and Engineering Research Council and Contract DAJA45-85-C-0028 from the US Army.

REFERENCES

1. A. Labeyrie, Astron and Astrophys, Vol 6, pp 85-87, (1970).
2. J. W. Goodman, in Laser Speckle and Related Phenomena, edited by J C. Dainty, Springer-Verlag, pp 9-75, (1984).
3. D. Korff, J. Opt. Soc. Am., Vol 63, pp 971-980, (1973).
4. J. C. Dainty in Ref. 2, pp 255-320.
5. H. Stark (editor), Image Recovery: Theory and Application, Academic Press, (1987).
6. C. R. Lynds, S. P. Worden and J. W. Harvey, Astrophys. J., Vol 207, pp 174-180, (1976).
7. R. H. T. Bates and F. M. Cady, Opt. Commun., Vol 32, pp 365-369, (1980).
8. F. M. Cady and R. H. T. Bates, Opt. Lett., Vol 5, pp 438-440, (1980).
9. A M. Sinton, B. L. K. Davey and R. H. T. Bates, J. Opt Soc. Am., Vol A3, 1010-1017, (1986).
10. J. C. Christou et al, Opt. Engng., Vol 25, pp 724-730, (1986).
11. B. R. Hunt, W. R. Fright and R. H. T. Bates, J Opt Soc. Am, Vol 73, pp 456-465, (1983).
12. L. C. de Freitas et al, this Proceedings.
13. J. G. Walker, Optica Acta, Vol 28, pp 735-738, (1981)
14. J. G. Walker, Appl. Opt., Vol 21, pp 3132-3137, (1982).
15. K. T. Knox and B. J. Thompson, Astrophys. J., Vol 193, pp L45-48, (1974)
16. M. P. Rimmer, Appl Opt., Vol 13, pp 623-629, (1974).
17. B. R. Hunt, J. Opt. Soc. Am., Vol 69, pp 393-399, (1979).
18. G. Weigelt, Opt Commun., Vol 21, pp 55-59, (1977).
19. A. W. Lohmann, G. Weigelt and B. Wirnitzer, Appl Opt., Vol 22, 4028-4037, (1983).
20. H. Bartelt, A. W. Lohmann and B. Wirnitzer, Appl. Opt, Vol 23, 3121-3129, (1984).
21. A. W. Lohmann and B. Wirnitzer, Proc. IEEE, Vol 72, pp 889-901, (1984).
22. G. R. Ayers, M. J. Northcott and J. C. Dainty, in preparation for J Opt. Soc. Am.
23. J. W. Goodman and J. F. Belsher, Proc. SPIE, Vol 75, pp 141-154, (1976)
24. P. Nisenson and C. Papaliolios, Opt. Commun., Vol 47, pp 91-96, (1983).

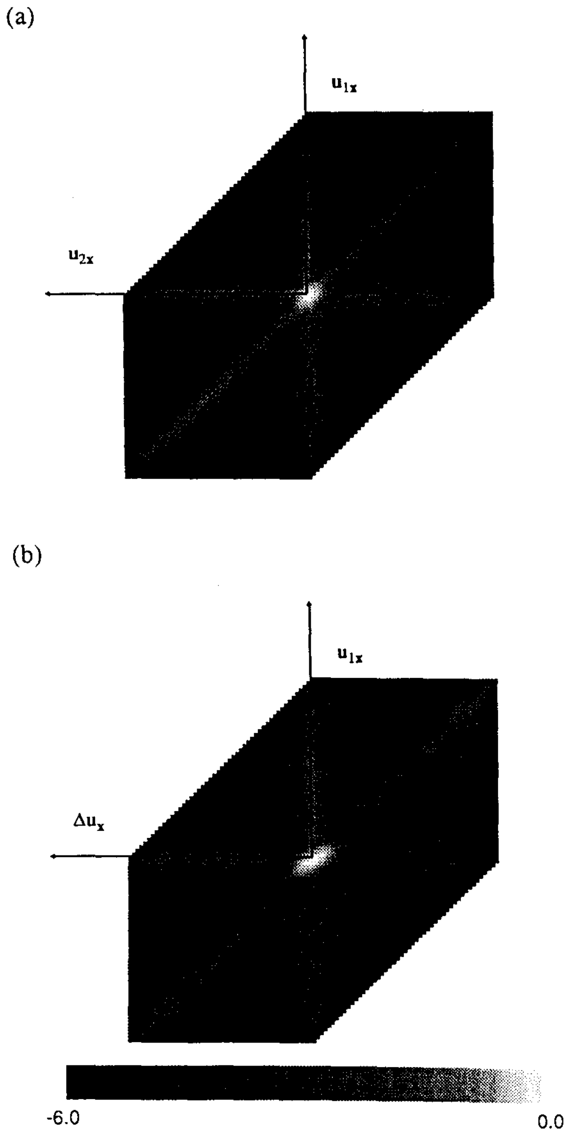

Figure (1)

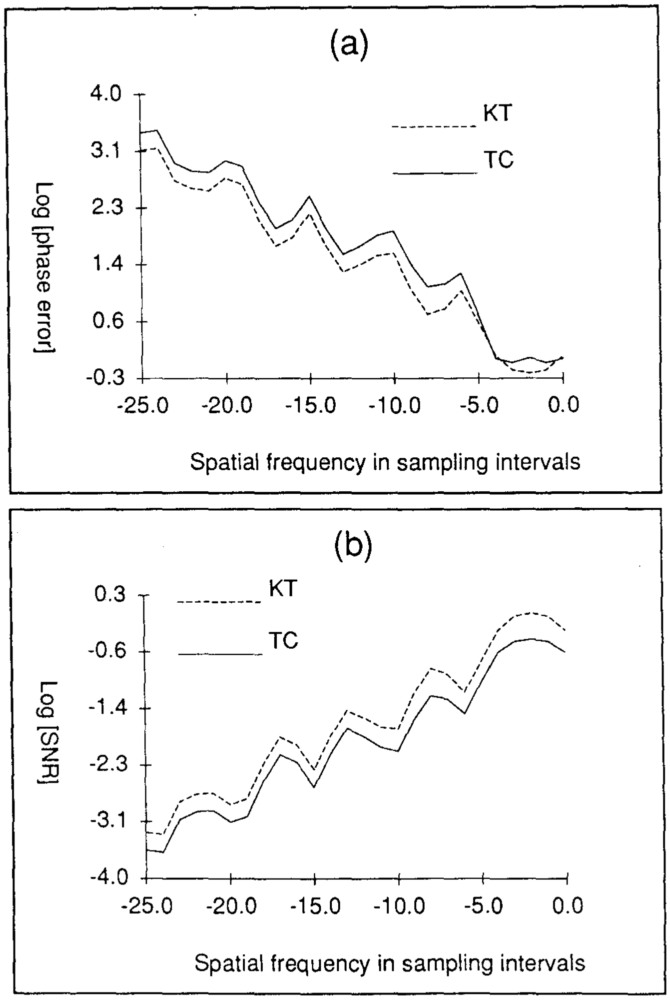

Figure (2)